Article

The Factor VII Variant p.A354V-p.P464Hfs: Clinical versus Intracellular and Biochemical Phenotypes Induced by Chemical Chaperones

Elisabeth Andersen [1,2,*], Maria Eugenia Chollet [1,2], Francesco Bernardi [3], Alessio Branchini [3], Marcello Baroni [3], Guglielmo Mariani [4,5], Alberto Dolce [6], Angelika Batorova [7], Ellen Skarpen [8], Christiane Filion Myklebust [1,2], Grethe Skretting [1,2] and Per Morten Sandset [1,2,9,*]

1   Department of Haematology, Oslo University Hospital, 0316 Oslo, Norway;
    m.e.c.dugarte@ous-research.no (M.E.C.); cfil.mykle@outlook.com (C.F.M.); grethe.skretting@gmail.com (G.S.)
2   Research Institute of Internal Medicine, Oslo University Hospital, 0372 Oslo, Norway
3   Department of Life Sciences and Biotechnology and LTTA Centre, University of Ferrara, 44121 Ferrara, Italy;
    francesco.bernardi@unife.it (F.B.); alessio.branchini@unife.it (A.B.); marcello.baroni@unife.it (M.B.)
4   Faculty of Science and Technology, Westminster University, London W1B 2HW, UK;
    Guglielmo.mariani189@gmail.com
5   Seven Treatment Evaluation Registry [STER] Study Group, 0316 Oslo, Norway
6   National Institute of Statistics, 90100 Palermo, Italy; Dolce@istat.it
7   The National Haemophilia Centre, Institute of Haematology and Blood Transfusion, School of Medicine of
    Comenius University, University Hospital, 813 72 Bratislava, Slovakia; batorova@npba.sk
8   Core Facility for Advanced Light Microscopy, Institute for Cancer Research, Oslo University Hospital,
    0379 Oslo, Norway; ellen.skarpen@rr-research.no
9   Institute of Clinical Medicine, University of Oslo, 01316 Oslo, Norway
*   Correspondence: elisabeth.andersen@gmail.com (E.A.); p.m.sandset@medisin.uio.no (P.M.S.);
    Tel.: +47-993-21-081 (E.A.); +47-975-91-745 (P.M.S.)

Abstract: (1) Background: Congenital factor (F) VII deficiency is caused by mutations in the *F7* gene. Patients with modest differences in FVII levels may display large differences in clinical severity. The variant p.A354V-p.P464Hfs is associated with reduced FVII antigen and activity. The aim of the study was to investigate the clinical manifestation of this variant and the underlying molecular mechanisms. (2) Methods: Analyses were conducted in 37 homozygous patients. The recombinant variant was produced in mammalian cells. (3) Results: We report a large variation in clinical phenotypes, which points out genetic and acquired components beyond *F7* mutations as a source of variability. In contrast, patients displayed similarly reduced FVII plasma levels with antigen higher than its activity. Comparative analysis of the recombinant variant and of plasma samples from a subset of patients indicated the presence of an elongated variant with indistinguishable migration. Treatment of cells with the chemical chaperone 4-phenylbutyrate (4-PBA) improved the intracellular trafficking of the variant and increased its secretion to the conditioned medium up to 2-fold. However, the effect of 4-PBA on biological activity was marginal. (4) Conclusions: Chemical chaperones can be used as biochemical tools to study the intracellular fate of a trafficking-defective FVII variant.

Keywords: factor VII deficiency; chemical chaperones; mutations; protein misfolding; endoplasmic reticulum; trafficking

1. Introduction

Factor (F) VII is a vitamin K-dependent glycoprotein synthesized in the liver that undergoes extensive post-translational modifications prior to secretion [1–3]. It is secreted into the blood where it circulates at a concentration of roughly 0.5 µg/mL (10 nM) [4]. The FVII protein contains an amino-terminal γ-carboxyglutamic acid domain followed by two epidermal growth factor (EGF)-like domains and a carboxy-terminal protease domain [5]. The single-chain native FVII is a zymogen that, upon binding to its cofactor,

tissue factor (TF), becomes activated, resulting in a two-chained activated molecule (FVIIa). The TF/FVIIa catalytic complex, which is considered the key initiator of blood coagulation, activates downstream clotting factors leading to the production of thrombin, the key effector for the final formation of the clot [6,7].

Congenital FVII deficiency (OMIM #227500) is a rare, autosomal recessive bleeding disorder caused by mutations in the *F7* gene resulting in a concomitant deficiency of plasma FVII protein (FVII antigen, FVII:Ag) and FVII procoagulant activity (FVII:C) (Type I deficiency) or in low FVII:C levels with normal, near-normal, or reduced FVII:Ag (Type II deficiency) [8]. In FVII deficiency, the spectrum of bleeding symptoms is widely variable [9,10]. Most patients exhibit mild symptoms such as mucocutaneous bleeds, whereas 10–15% of patients may experience potentially life-threatening hemorrhages such as central nervous system (CNS) or gastrointestinal (GI) bleeds [11–13]. The *F7* p.A354V-p.P464Hfs compound variant is caused by the p.A354V missense change, with pleiotropic effects in the FVII catalytic domain [14], and a cytosine deletion causing a frameshift at the C-terminal codon 464, which produces an elongated protein [15]. This variant represents the most frequent *F7* alteration in Central Europe [13,16–18] reported in the FVII variant database (https://f7-db.eahad.org/, accessed on 1 May 2021) [19] and is associated with a bleeding phenotype due to severely reduced FVII:C and FVII:Ag in plasma [16,20].

We previously reported minimal FVII secretion in cells expressing the recombinant (r) FVII p.A354V-p.P464Hfs (rFVII-354V-464Hfs) variant [21,22], resembling the patient phenotype. Our data suggested that the combined protein alterations were associated with a defective folding and that the misfolded state led to impaired trafficking, endoplasmic reticulum (ER) retention and ER stress. Very few studies on the clinical manifestations of the p.A354V-p.P464Hfs variant have been performed with a small number of patients [13,16], and detailed studies on the residual activity of this variant are hampered by the low levels of FVII in plasma and very reduced secretion after recombinant expression [13]. The relatively high frequency for a symptomatic mutation in a rare bleeding disorder, as well as the presence of small amounts of residual activity of this variant, provides a unique opportunity to investigate, in a constant *F7* mutation background, the poor consistency between FVII levels and the clinical manifestations, a key issue in FVII deficiency [23]

In the present study, we collected and analyzed data on FVII plasma activity and bleeding phenotype in 37 p.A354V-p.P464Hfs homozygotes as a means to deepen our knowledge on the genotype–plasma and clinical phenotype relationships. The rFVII-354V-464Hfs was produced in Chinese hamster ovary (CHO) K1 cells and compared to patient phenotypes and plasma FVII from a subset of patients. We recently demonstrated that the chemical chaperone 4-phenylbutyrate (4-PBA) could improve the secretion and biological activity of another recombinant FVII variant characterized by impaired secretion and triggering of ER stress [24]. Thus, we aimed to increase the expression of rFVII-354V-464Hfs and also to investigate the effect of chemical chaperones on intracellular processing and secretion, as well as on the catalytic activity of the secreted variant.

2. Materials and Methods

2.1. Nomenclature

Amino acid positions are reported in accordance with the Human Genome Variation Society (HGVS) nomenclature, whose numbering begins with the AUG translation initiation codon as position +1 [25,26].

2.2. Patients

The Seven Treatment Evaluation Registry (STER) prospectively collected data on bleeding episodes, surgery or prophylaxis in patients with FVII deficiency following strictly controlled data collection procedures established by the International FVII Deficiency Study Group [11]. We used the detailed data captured in STER to investigate the plasma and bleeding phenotypes of the p.A354V-p.P464Hfs variant in patients. At enrolment, a blood sample was drawn for centralized plasma inhibitor determination [27].

2.3. Cell Lines and Transfection

CHO-K1 cells (CCL61, American Type Culture Collection, Manassas, VA, USA) were cultured in Dulbecco's modified Eagle medium (DMEM, Lonza Group Ltd., Basel, Switzerland) supplemented with 10% fetal bovine serum (Hyclone FBS, GE Healthcare, Boston, MA, USA), 1% penicillin/streptomycin (Lonza Group Ltd., Basel, Switzerland) and 0.07 g/L L-Proline (Sigma Aldrich, Saint Louis, MO, USA) in a humidified atmosphere at 5% CO_2. The day before transient transfection, cells were seeded at an appropriate density to reach 50–80% confluency at the time of transfection on CELLBIND plates (Corning Incorporated, Kennebunk, ME, USA) or chambers slides (Ibidi GmbH, Gräfelfing, Germany). The plasmid vectors (pcDNA 3.1, Thermo Fisher Scientific, Rockford, IL, USA) containing *F7* cDNA coding for wild-type (wt) or p.A354V-p.P464Hfs FVII were generated as previously described [13,28]. The empty vector without insert was used as negative control in the experiments. Plasmid DNA was introduced into the cells by lipid transfection (Lipofectamine LTX, Thermo Fisher Scientific, Rockford, IL, USA) according to the manufacturer's protocol. CHO-K1 cells with stable expression of rFVIIwt or rFVII-354V-464Hfs were generated as previously described [24].

2.4. Treatment with Chemical Chaperones

CHO-K1 cells with stable or transient rFVII expression were treated with 0, 5, 7.5 or 10 mM 4-PBA (SML0309, Sigma Aldrich, Saint Louis, MO, USA) or 0, 25 or 50 μM binding immunoglobulin protein (BiP) protein inducer X (BIX;SML1073, Sigma Aldrich, Saint Louis, MO, USA) diluted in DMEM with 1% FBS and 10 μg/mL Vitamin K (V3501, Sigma Aldrich, Saint Louis, MO, USA) for 48 h.

2.5. Gene Expression Analysis

Total RNA was isolated from cells using the MagMAX-96 Total RNA Isolation Kit (Thermo Fisher Scientific, Rockford, IL, USA) on a MagMAX particle processor (Thermo Fisher Scientific, Rockford, IL, USA). cDNA was synthesized using the High-Capacity cDNA Reverse Transcription Kit (Thermo Fisher Scientific, Rockford, IL, USA). Taqman quantitative reverse transcriptase PCR (qRT-PCR) was performed using the following Taqman assays: Hs01551992_m1 (*F7*), Rn99999125_m1 (*BCL-2*), Hs99999001 (*BAX*) and Hs99999901_s1 (*18S*) (all from Thermo Fisher Scientific, Rockford, IL, USA). To determine the mRNA levels of spliced and unspliced X-box binding protein 1 (*sXBP1* and *uXBP1*, respectively), SYBR green primers were designed as previously described [22]. Eukaryotic 18S ribosomal RNA (*18S*) (forward primer: 5′-CGGACAGGATTGACAGATTG-3′, reverse primer: 5′-CAAATCGCTCCACCAACTAA-3′) was used as endogenous control. SYBR green qRT-PCR was performed using the Power SYBR Green PCR Master Mix (Thermo Fisher Scientific, Rockford, IL, USA) on a 7900HT Fast Real-Time PCR system.

2.6. ELISA

After treatment with chemical chaperones, the conditioned medium was harvested from cells. The cells were then washed briefly with ice-cold phosphate-buffered saline (PBS) before lysis in RIPA buffer (Sigma Aldrich, Saint Louis, MO, USA) supplemented with 1x Halt protease and phosphatase inhibitor cocktail (Thermo Fisher Scientific, Rockford, IL, USA). The conditioned medium and the lysates were precleared by centrifugation (15 min/18.200 rcf and 10 min/8000 rcf, respectively). FVII antigen (FVII:Ag) in the conditioned medium and in the cell lysates was measured using the VisuLize FVII ELISA (detection limit: <0.01 IU/mL (5 ng/mL; <1%)), Affinity Biologicals, Ancaster, ON, Canada) on a SpectraMax Plus spectrophotometer (Molecular Devices, Sunnyvale, CA, USA). Total protein in cell lysates was assessed using the Pierce BCA protein assay kit (Thermo Fisher Scientific, Rockford, IL, USA).

2.7. SDS-PAGE and Western Blot Analysis

Plasma or cell lysates were diluted 1:40 in HEPES-buffered saline (Sigma Aldrich). For analysis of ER chaperone proteins, an equal amount of protein from the cell lysates was diluted in RIPA buffer. The proteins were denatured for 4 min at 95 °C using the Lane Marker Reducing Sample Buffer (DTT, 5 x concentrate, Thermo Scientific). The samples were separated on 10% Mini-PROTEAN TGX gels (Bio-Rad, Hercules, CA, USA) and transferred onto Sequi-Blot PVDF membranes (Bio-Rad, Hercules, CA, USA). The membranes were blocked with nonfat dry milk (Bio-Rad, Hercules, CA, USA) before incubation overnight at 4 °C with primary antibodies against FVII (goat polyclonal; R&D systems, Minneapolis, MN, USA), BiP (rabbit monoclonal; Cell Signaling Technology, Danvers, MA, USA), glucose-regulated protein 94 (GRP94) (rabbit polyclonal; Cell Signaling Technology, Danvers, MA, USA) or β-actin (rabbit polyclonal; Cell Signaling Technology Danvers, MA, USA). The membranes were briefly washed with Tris-buffered saline containing 1% Tween-20 before incubation for 1 h with the appropriate HRP-linked secondary antibodies (donkey anti-goat, Santa Cruz Biotechnology, Dallas, TX, USA, or goat anti-rabbit, Cell Signaling Technology, Danvers, MA, USA). Membranes were visualized by the addition of a chemiluminescent substrate (Radiance Plus, Azure Biosystems, Dublin, CA, USA), and images were acquired on a biomolecular imager (ImageQuant LAS 4000 Mini, GE Healthcare, Chicago, IL, USA). The rFVIIwt or normal plasma from a healthy donor were used as controls for the expressed rFVII-354V-464Hfs variant or patient plasma samples, respectively.

2.8. Generation of Activated FX in Medium

Cells with stable expression of rFVIIwt or rFVII-354V-464Hfs were seeded onto 15 cm dishes (Thermo Scientific, Rockford, IL, USA) and treated with ± 10 mM 4-PBA. Conditioned medium was harvested and concentrated approximately 30 times through the Amicon Ultra Centrifugal Filter devices (cut-off 10 kDa, Millipore, Carrigtwohill, Country Cork, Ireland). Generation of activated factor X (FXaG) was performed in FVII-deficient plasma (HemosIL®, Instrumentation Laboratory, Bedford, MA, USA) added with the concentrated medium from transfected cells. The assay was performed in an HBS buffer (Hepes, 20 mM; NaCl, 150 mM; PEG-8000, 0.1%; pH 7.4) as previously described [29]. Briefly, after incubation for 3 min at 37 °C, FXaG was triggered by 50 pM Tissue Factor (Innovin, Dade Behring, Marburg, Germany) and evaluated by adding a specific FXa fluorogenic substrate (Spectrafluor FXa, American Diagnostica, Stamford, CT, USA). FXaG was also evaluated by inhibition of tissue factor pathway inhibitor (TFPI) by anti-TFPI RNA aptamer (5′-GGAAUAUAdCUUGGdCUdCGUUAGGUGdCGUAUAUAidT-3′), as previously described [30,31].

2.9. Immunostaining and Confocal Microscopy

Immunostaining was performed by using antibodies against FVII (rabbit polyclonal, Novus biologicals, Centennial, CO, USA, or goat polyclonal, R and D Systems), the ER marker protein disulfide isomerase (PDI; Enzo Life Sciences, Farmingdale, NY, USA), the Golgi marker GM130 (BD Biosciences, San Jose, CA, USA), the *trans*-Golgi network marker TGN46 (Novus biologicals, Centennial, CO, USA), Golgi reassembly stacking protein (GRASP) 55 (Santa Cruz Biotechnology, Dallas, TX, USA), GRASP 65 (Novus biologicals, Centennial, CO, USA), ras-related protein (Rab)-11 (BD Biosciences), Rab-8 (LifeSpan BioSciences, Seattle, WA, USA), coat protein (COP) II (Thermo Fisher Scientific, Rockford, IL, USA), ER-Golgi intermediate compartment (ERGIC)-53 (Santa Cruz Biotechnology, Dallas, TX, USA), LC3 (MBL Woburn, MA, USA) and Golgi subfamily B member 1 Giantin (BioLegend, San Diego, CA, USA). The Alexa Fluor® 488 donkey anti-goat (Thermo Fisher Scientific, Rockford, IL, USA), Alexa Fluor® 488 donkey anti-rabbit (Thermo Fisher Scientific, Rockford, IL, USA), Alexa Fluor® 568 donkey anti-mouse (Thermo Fisher Scientific, Rockford, IL, USA), or Alexa Fluor® 568 donkey anti-rabbit (Thermo Fisher Scientific, Rockford, IL, USA) were used as secondary antibodies. The cells were imaged as previously described [24]. Negative controls with only secondary antibodies, as well as double

negative controls using one of the primary antibodies and both secondary antibodies, were included.

2.10. Data Analysis

The statistical analyses were performed using GraphPad Prism 8.0.1 (Graphpad Holdings, LLC, San Diego, CA, USA). Comparisons were performed using one-way ANOVA or Welch's *t*-test. A *p*-value of ≤0.05 was considered statistically significant. FXaG parameters were extrapolated from the first derivative of relative fluorescence units (RFU) as a function of time (minutes) [29].

3. Results

3.1. Bleeding and Plasma Phenotypes in Patients

First, the most relevant information about symptoms and clotting phenotypes in the 37 selected individuals was analyzed. The type and prevalence of symptoms in the 35 symptomatic p.A354.p.P464Hfs homozygotes are summarized in Figure 1A together with age at first symptom, a parameter contributing to defining the degree of bleeding severity in patients. The group includes patients ranging from asymptomatic (*n* = 2) to patients who experienced hemarthrosis (*n* = 6). This variability is also supported by the age at first symptom (Figure 1A, left panel). Whereas the median age of the first symptom (six years) defines a moderate to mild condition, two patients experienced bleeding before reaching one year, which is a frequent observation in severe FVII deficiency (Figure 1A, right panel). Figure 1B summarizes the plasma phenotype in terms of FVII:C and FVII:Ag for this mutation. These data define a potentially severe defect with a median FVII:C value slightly exceeding 1% of normal levels. The distribution of FVII:Ag and FVII:C/FVII:Ag (C/Ag) ratio, from a proportion of the patients (*n* = 28, Figure S1), indicates that the p.A354.p.P464Hfs activity was more reduced than its antigen levels in most patients, with a median FVII:Ag value and C/Ag ratio of approximately 1.8% and 0.6, respectively.
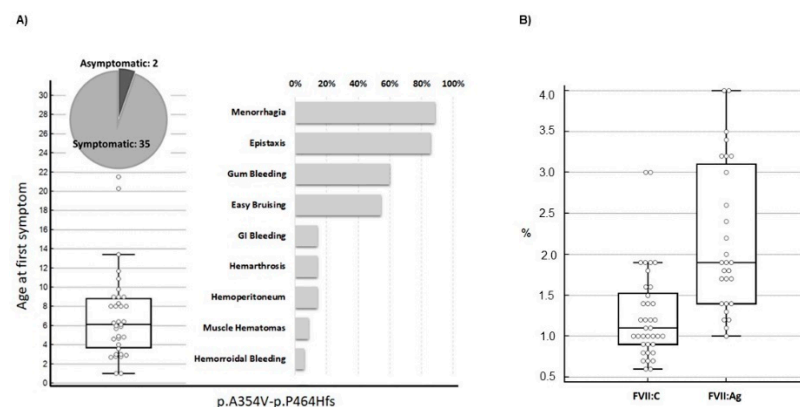

Figure 1. Clinical presentation in homozygous patients for the p.A354.p.P464Hfs mutation. (**A**) Age at first symptom and prevalence of type of hemorrhage in patients homozygous (*n* = 37, females *n* = 26) for the compound p.A354.-p.P464Hfs mutation. Symptom prevalence is reported in relation to the number of symptomatic homozygotes (*n* = 35). Menorrhagia prevalence is indicated in relation to female homozygotes. (**B**) FVII activity (*n* = 37) and FVII antigen (*n* = 28) values in the p.A354.p.P464Hfs homozygotes. Data are presented as box plots. FVII:Ag, FVII antigen; FVII:C, FVII procoagulant activity.

3.2. Comparison of Plasma and Recombinant FVII Variants

The FVII p.A354V-p.P464Hfs variant is characterized by a missense change (A354V) and a cytosine deletion at the C-terminal codon 464 resulting in a frameshift and the production of an elongated protein (Figure 2A). We compared the protein variant from patients' plasma with that expressed in eukaryotic cells (Figure 2B). Plasma samples from unrelated patients were compared with normal plasma or rFVIIwt from cell lysates by

SDS-PAGE followed by Western blotting analysis using a polyclonal anti-FVII antibody. The FVII variant in plasma migrated slightly slower than rFVIIwt and FVII from normal plasma, confirming the presence of the elongated protein with a higher molecular weight. The plasma variant migrated similarly to rFVII-354V-464Hfs.
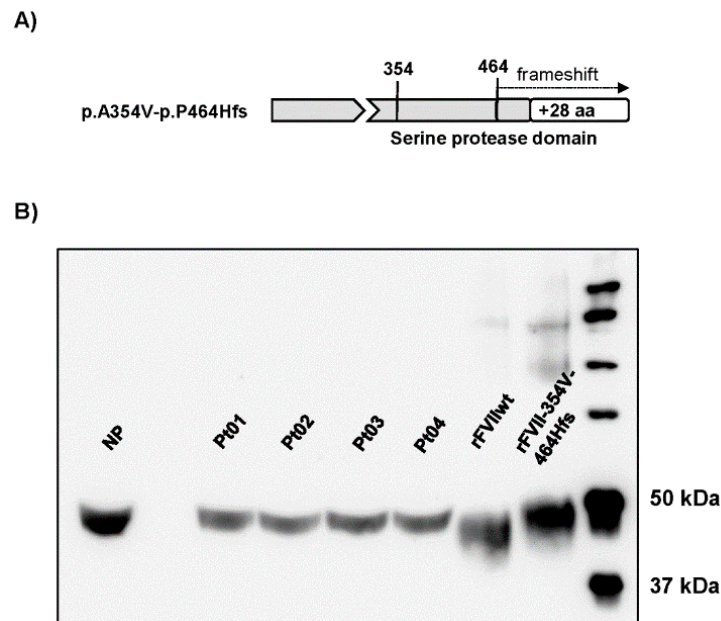
Figure 2. FVII protein forms in patients' plasma and upon recombinant expression. (**A**) Schematic representation of the FVII p.A354V-p.P464Hfs variant. (**B**) Western blot analysis (image adjusted for brightness/contrast) of FVII in plasma from the four patients (Pt 01–04), a healthy volunteer (normal plasma, NP) or cell lysates from cells with stable expression of rFVIIwt or rFVII-354V-464Hfs.

3.3. The Effect of Chaperone Treatment on FVII Variant Biosynthesis and Secretion

FVII:Ag levels were measured in conditioned medium and in cell lysates from cells treated with chemical chaperones. In cells treated with 4-PBA, the secreted amounts of rFVII-354V-464Hfs increased ~2.5-fold, while intracellular levels of the rFVII-354V-464Hfs were increased ~2-fold compared to untreated cells (Figure 3A). Treatment with BIX had a modest although statistically significant effect on secretion of the rFVII-354V-464Hfs (approximately 1.3-fold at the highest concentration), whereas the intracellular levels of the variant were increased up to ~2.3-fold at the highest concentration (Figure 3B). Because we observed that treatment with the chemical chaperones also increased the FVII:Ag levels in cell lysates, a ratio between secreted (conditioned medium) and intracellular (lysates) FVII was calculated. The secreted/intracellular ratio in cells treated with 4-PBA was increased up to 2-fold compared to untreated cells (Figure 3C). However, the ratio was decreased 0.7-fold and 0.6-fold in cells treated with 25 or 50 μM BIX, respectively, compared to untreated cells (Figure 3D). We found no significant effect of BIX on rFVIIwt secreted to the conditioned medium, but a small increase of rFVIIwt was measured in cell lysates at the highest BIX concentration (Figure S2).
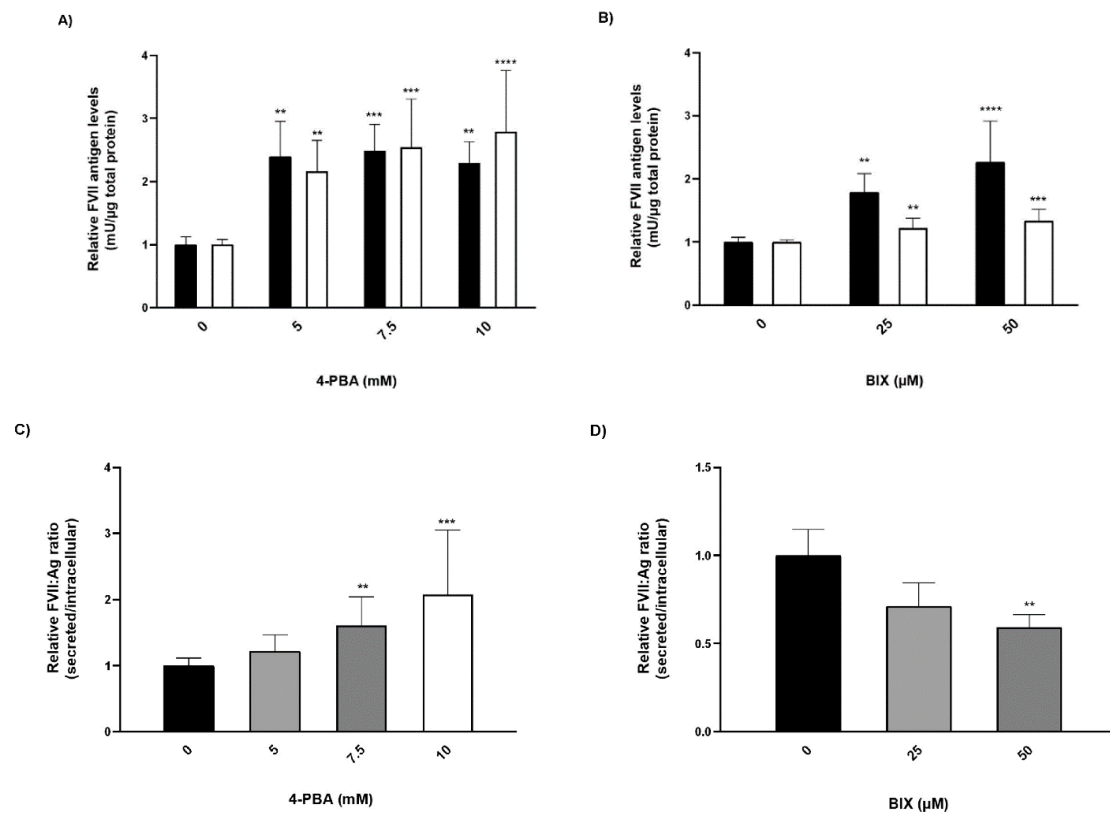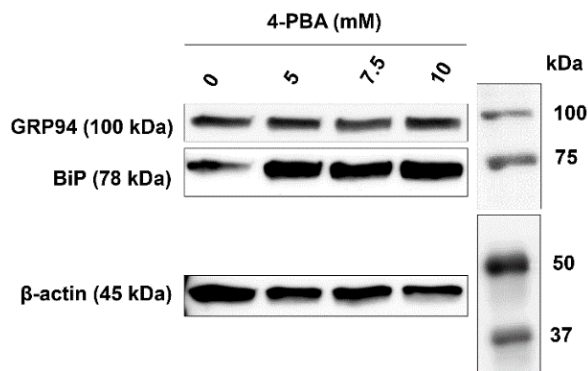
Figure 3. The effect of chaperone treatment on FVII variant production and secretion. Cells with stable expression of rFVII-354V-464Hfs were treated with 4-PBA or BIX for 48 h. (**A**,**B**) FVII:Ag levels in medium (white bars) or cell lysates (black bars). To adjust for variations in cell number, the FVII:Ag levels were adjusted to the corresponding total protein content in the respective wells. (one-way ANOVA, **** $p \leq 0.0001$, *** $p \leq 0.001$, ** $p \leq 0.01$). (**C**,**D**) Ratio between the secreted versus intracellular FVII:Ag. Values are expressed relative to untreated cells and are reported as mean ± SD from at least three independent experiments performed in duplicate (**** $p \leq 0.0001$, *** $p \leq 0.001$, ** $p \leq 0.01$; one-way ANOVA).
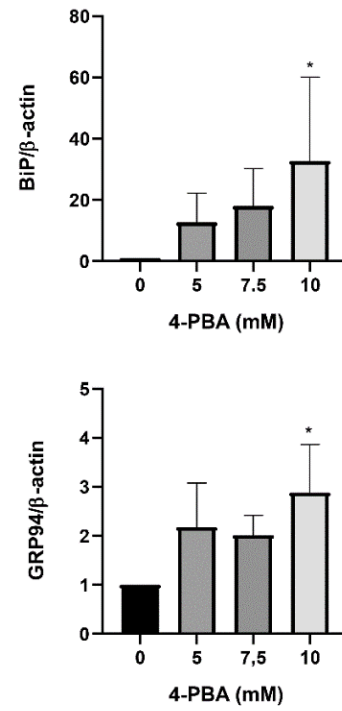
3.4. The Effect of Chaperone Treatment on the ER Folding Machinery

Because the chaperone treatment increased the levels of the rFVII variant, its effect on the ER folding machinery was assessed. Protein expression of the ER chaperones BiP and GRP94 was analyzed by Western blot. In cells treated with 4-PBA, the protein levels of BiP and GRP94 were increased up to approximately 30-fold and 3-fold, respectively, at the highest concentration (Figure 4A,B). In cells treated with BIX, the levels of BiP were increased approximately 5-fold at the highest concentration, whereas no statistically significant differences in the levels of GRP94 were observed (Figure 4C,D). Moreover, the levels of spliced (s) X-BOX binding protein (XBP1) mRNA, a transcription factor that regulates ER chaperone genes, were increased approximately 1.5-fold in cells treated with the highest concentration of 4-PBA and BIX, respectively (Figure 4E,F). An overload of the folding machinery and ER stress can induce apoptosis, and we therefore investigated the effect of different doses of the chaperones on the expression of the pro- and antiapoptotic genes BAX and BCL-2. We measured a >50% reduction in the ratio of proapoptotic BAX versus antiapoptotic BCL-2 mRNA in cells treated with 4-PBA, whereas in cells treated with BIX an increased ratio was observed (Figure S4A,B). There was no dose–response with either chaperone.
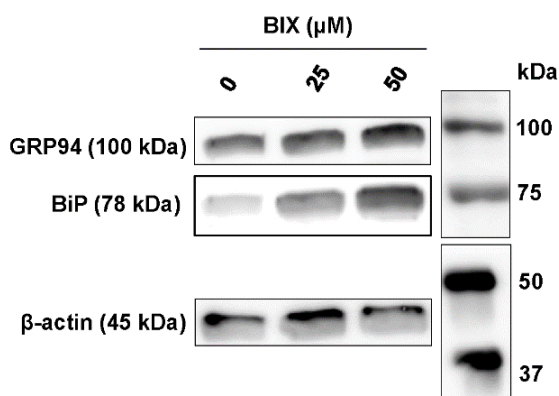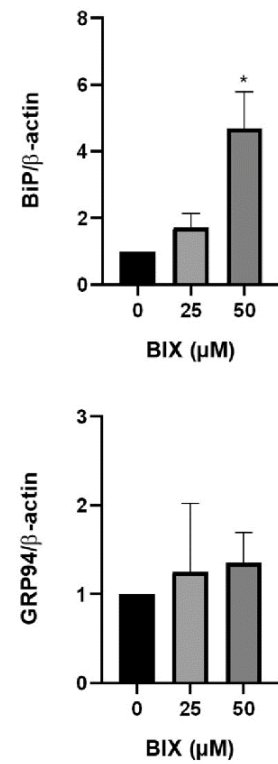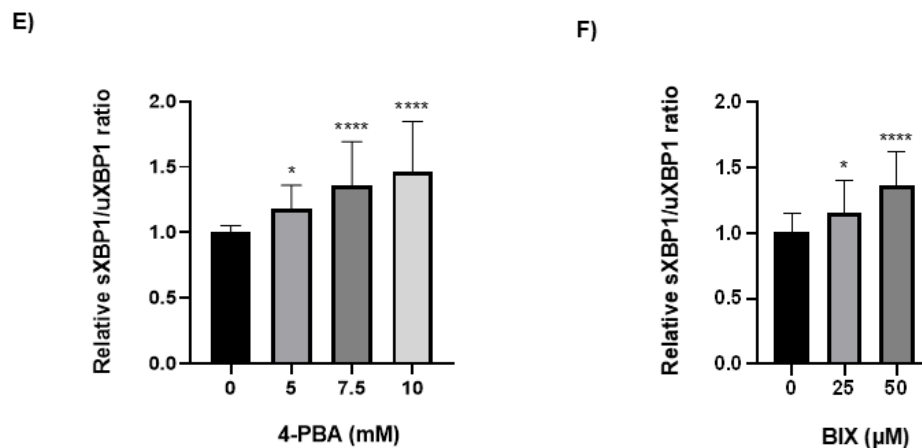
A)

B)


C)

D)

Figure 4. *Cont.*

E)

F)

Figure 4. The effect of chaperone treatment on the ER folding machinery. (**A**) Representative Western blot analysis (cropped image adjusted for brightness/contrast) of lysates from cells treated with 4-PBA for the detection of BiP and GRP94. β-actin was used as loading control. (**B**) Densitometric analysis of bands from (**A**), representing BiP or GRP94 normalized to β-actin. (**C**) Representative Western blot analysis (cropped image adjusted for brightness/contrast) of lysates from cells treated with BIX for the detection of BiP and GRP94. β-actin was used as loading control. (**D**) Densitometric analysis of bands from (**C**), representing BiP or GRP94 normalized to β-actin. (**E,F**) mRNA levels of sXBP1 and uXBP1 were assessed by SYBR green qRT-PCR. Quantitation was performed using the comparative CT method with 18S as the endogenous control gene and untreated cells as the calibrator. Values are shown as mean ± SD of fold change relative to untreated cells from three independent experiments. **** $p \leq 0.0001$, * $p \leq 0.05$ (one-way ANOVA).

### 3.5. Intracellular Localization Studies

Because a net effect on secretion of the FVII variant could only be observed in cells treated with 4-PBA, we next investigated whether the treatment with this compound could have an impact on intracellular trafficking. Cells were stained with markers for different organelles and vesicles and analyzed by immunofluorescence. After treatment with 4-PBA, we observed an increased colocalization with the *trans*-Golgi network marker TGN46 and the vesicle marker COPII, but not with the Golgi marker GM130 (Figure 5A). Analysis of Pearson's correlation coefficient demonstrated a significantly increased colocalization of the rFVII-354V-464Hfs with TGN46 in cells treated with 4-PBA compared to untreated (control) cells, whereas the correlation coefficient for COPII did not reach statistical significance (Figure 5B,C). We also observed an increased but not statistically significant colocalization of FVIIwt with TGN46 and COPII after treatment with 4-PBA (Figure S5). No colocalization with other markers, such as the Golgi reassembly stacking proteins GRASP55 or GRASP65, the endosomal markers Rab-8 or Rab-11 or the autophagosomal marker LC3II was observed (Figure S6).
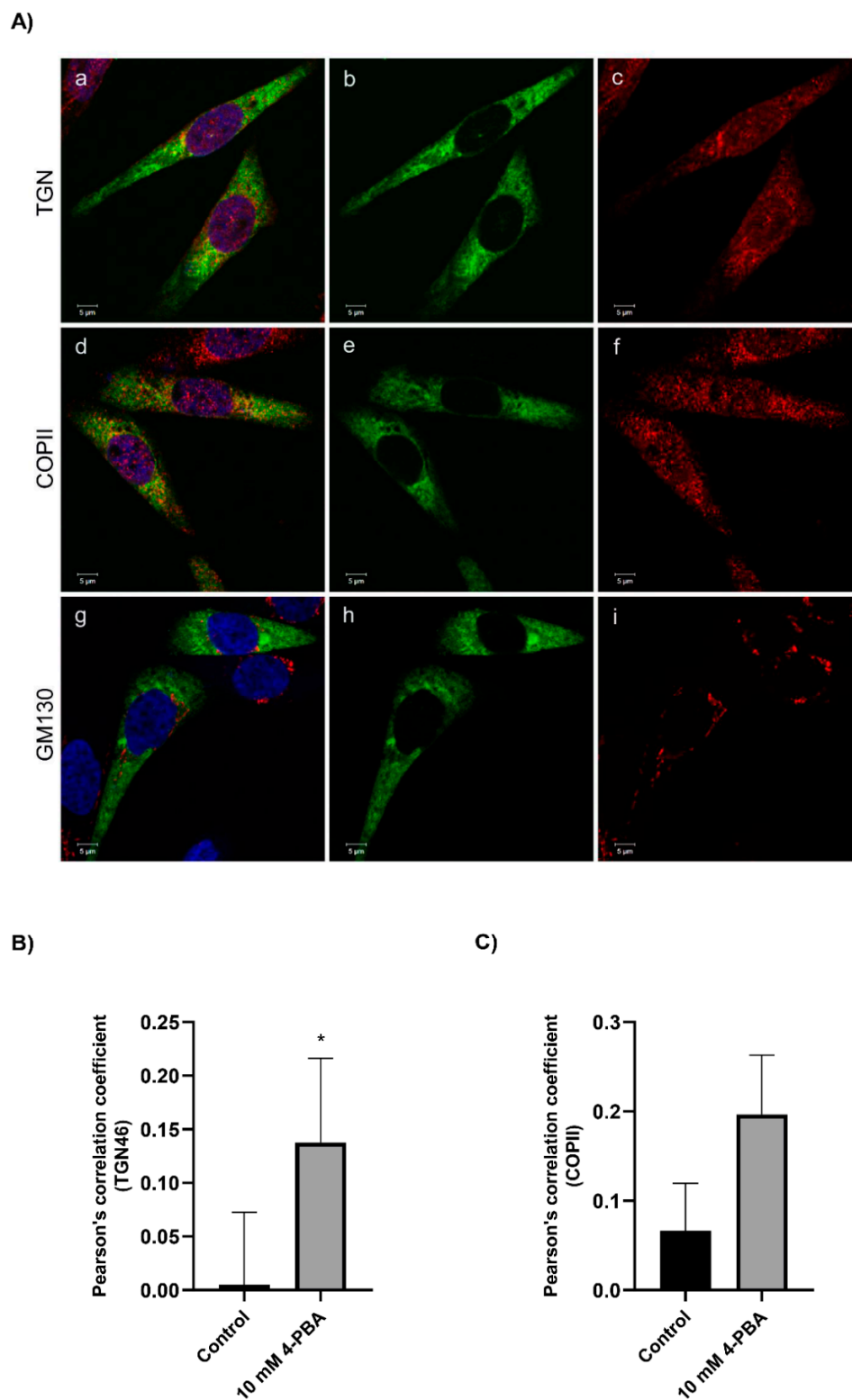
Figure 5. The effect of 4-PBA treatment on intracellular localization of the rFVII-354V-464Hfs variant. (**A**) Confocal images from cells treated with 4-PBA costained with FVII and membrane organelle markers GM130, COPII or TGN46. Cells with transient expression of rFVII-354V-464Hfs were treated with 4-PBA for 42 h. Confocal images from cells stained with FVII (green, b, e, h) and membrane organelle marker (GM130, COPII or TGN46, red, c, f, i). Colocalized green and red pixels are shown in yellow color (a, d, g). Bar: 5 μm. (**B**) The colocalization of FVII with TGN46 (**B**) and COPII (**C**) was calculated by Pearson's correlation coefficient in untreated (control) cells and cells treated with 4-PBA. Results are presented as the mean $\pm$ SD of four independent experiments (*t*-test). * $p < 0.05$.

3.6. The Effect of 4-PBA Treatment on Biological Activity of FVII

The evaluation of the biological activity of the secreted FVII variant after treatment was restricted to the samples from cells treated with 4-PBA. Considering the pivotal role of activated FVII in coagulation initiation, as well as in the conversion of zymogen FX into activated FX (FXa), the ability of the FVII variant to generate FXa (FXaG) was measured. Measurements were performed in FVII-deficient plasma with the addition of concentrated medium from cells treated or untreated with 4-PBA. The FVII:Ag measured in media after the concentration procedure was 73.8 ng/mL. A high concentration (50 pM) of TF, the essential FVII cofactor, was used to magnify the modest residual activity of the rFVII-354V-464Hfs variant. We evaluated the peak parameter of FXaG, which reflects FVIIa activity (Figure 6) [29]. Upon treatment, the peak was much higher than in the absence of 4-PBA (44 RFU/s vs. 15.5 RFU/s, respectively). The time needed to reach the peak of fluorescence (time to peak) was also shortened (315 s vs. 375 s, respectively) (Figure 6).
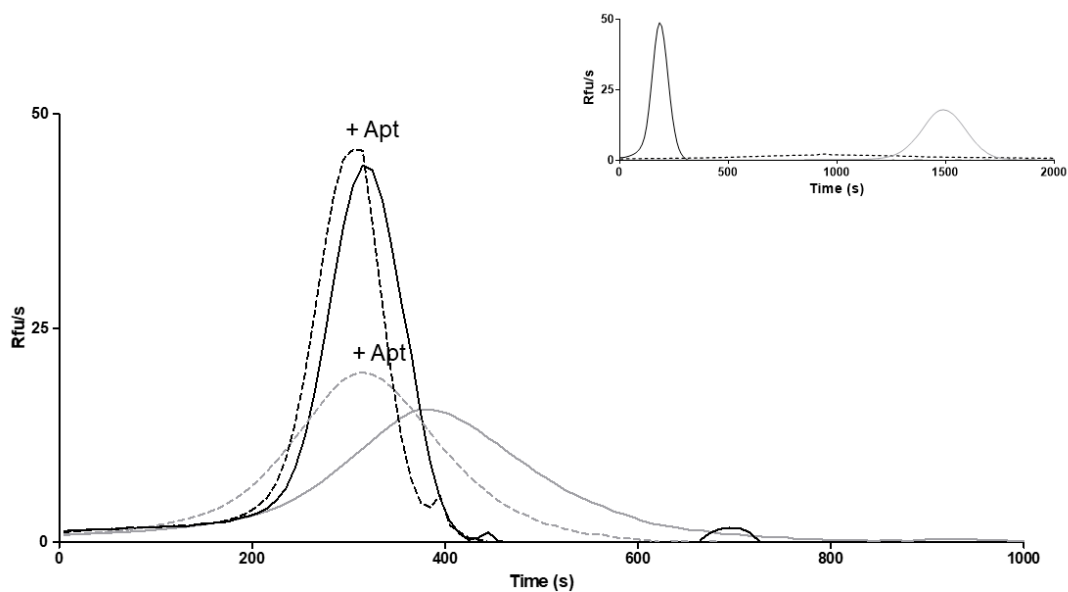
Figure 6. FXa generation in medium from cells treated with 4-PBA. FXa generation activity in FVII-deficient plasma added with medium from 4-PBA treated cells (continuous black line) and untreated (continuous gray line) cells, or in the presence of anti-TFPI aptamer (+Apt) in medium from 4-PBA treated (dotted black line) and untreated (dotted gray line) cells. RFU/s, relative fluorescence units/second. Inset: curves obtained with diluted (0.1%) medium containing rFVIIwt (black line), vector alone (dotted line) or FVII-deficient plasma alone (gray line).

To deepen our knowledge on FXaG by rFVII-354V-464Hfs, we inhibited tissue factor pathway inhibitor (TFPI), the main physiological inhibitor in the TF-initiated coagulation pathway, using an anti-TFPI aptamer (Figure 6). TFPI inhibition is expected to magnify FXaG. Accordingly, inhibition of TFPI increased FXaG activity of the 4-PBA-induced FVII variant and in medium from untreated cells.

4. Discussion

The p.A354V-p.P464Hfs variant represents a paradigmatic model mutation in FVII deficiency, both on studies of bleeding phenotype and on the molecular mechanisms underlying FVII deficiency. Among the large number of coagulation protein variants, only protein C Nagoya, a thrombophilic mutation, can be compared with *F7* p.A354V-p.P464Hfs, both in terms of molecular mechanisms (translation frameshift and elongated protein) and frequency [32]. In addition, a novel homozygous *F11* frameshift mutation resulting in an extended FXI carboxyl-terminus, ER retention and reduced secretion was recently identified in a Japanese patient [33].

The analysis of clinical phenotypes in 37 homozygotes for the p.A354V-p.P464Hfs variant significantly extends previous information about variability in bleeding severity in FVII-deficient patients. The small range of FVII:C in a group of patients with the same *F7* genotype supports the notion that a large variation in clinical phenotypes is detectable with relatively small variations in FVII activity, a major open question in FVII deficiency [3]. The investigation of FVII:Ag in plasma revealed that the antigen levels were clearly higher than the activity levels, suggesting a Type-II defect. The difference concerning the assay methods is relevant as the ELISA is indeed more sensitive and precise than the coagulation assay. However, both measurements display the same variability, suggesting a true variation between the studied individuals. Overall, findings in patients indicated that the elongated p.A354V-p.P464Hfs variant circulated in plasma at low but detectable concentrations. Its activity in plasma was reduced but detectable. Our study clearly suggests that yet unknown genetic and acquired components beyond *F7* mutations play a role in producing variability in clinical manifestations in this deficiency.

The recombinant expression of the p.A354V-p.P464Hfs variant was aimed at providing the molecular basis underlying these observations. The Western blot analysis of patient plasma demonstrated a band with a migration pattern that was slower than that of normal plasma FVII. This pattern, indicating a protein larger in size, is in agreement with the base-pair deletion at position 464, producing a frameshift mutation that results in additional 28 residues at the protein carboxyl-terminus [16]. In fact, the FVII in plasma from patients homozygous for the p.A354V-p.P464Hfs variant migrated in a comparable manner to that of rFVII-354V-464Hfs, suggesting a similar processing of this protein variant in the CHO-K1 cells. When FVII is overexpressed in CHO cells, it undergoes similar post-translational modifications as plasma-derived FVII, which makes these cells the best option for the production of rFVII [34].

Chemical chaperones are known to prevent misfolded protein aggregation and alleviate ER stress, thereby improving the biosynthesis of misfolded proteins [35,36]. We explored the possibility that the chaperone-based approach could potentiate folding and secretion of p.A354V-p.P464Hfs variant. This would unravel biological pathways that could participate in the secretion of small amounts of the variant, which is of utmost importance to modulate bleeding phenotypes in patients. Treatment with the chemical chaperones 4-PBA and BIX increased the levels of rFVII-354V-464Hfs in cell lysates and in the medium. However, a net effect on secretion could only be observed in cells treated with 4-PBA. We previously reported an effect of 4-PBA on the secretion of the FVII p.Q160R variant [24] and on a protein C variant [37], and similar results were reported for FIX in a cellular model of hemophilia B [38]. In the present study, we observed an increased colocalization with the *trans*-Golgi network marker TGN46 and with the vesicular marker COPII. The export of cargo out of the ER is mediated by COPII-coated vesicles that bud from the ER at ER-exit sites (reviewed in [39] and [40]), and the *trans*-Golgi network is a distinct membranous compartment at the *trans* face of the Golgi apparatus thought to be involved in the sorting of secretory proteins [41]. This could indicate that treatment with 4-PBA might facilitate transport out of the ER and into the secretory pathway, as reported for other FVII variants [24].

Our previous studies demonstrated increased ER stress in cells expressing rFVII-354VHfs and upregulation of the unfolded protein response [22]. In our model, 4-PBA and BIX increased the expression levels of the ER chaperone BiP, which can bind to exposed hydrophobic residues of unfolded proteins and plays a key role in protein folding and quality control in the ER [42]. In a recent study by Vitale et al., it was shown that inadequate BiP expression upon bulk expression of secretory immunoglobulin M heavy chain caused proteotoxicity [43]. The authors argued that pharmacological intervention against proteotoxicity should primarily be aimed at promoting a favorable level of BiP versus the client protein. For 4-PBA, the increase in BiP was accompanied by a reduced ratio of BAX/BCL-2, suggesting an antiapoptotic state in the cells supporting this hypothesis. In addition to increasing the levels of BiP, 4-PBA also increased the expression of the ER chaperone GRP94

and both chaperones increased the levels of the transcription factor sXBP1, which is known to increase the transcription of key ER chaperones. Based on these observations, we might hypothesize that the enhanced folding capacity of the ER following chaperone treatment contributes to the increased levels of the FVII variant in the cell lysates. Even small changes of folding capacity in the patients' hepatocytes would be candidates to produce the small differences observed in plasma p.A354V-p.P464Hfs levels among patients, which in turn could potentially contribute to producing differences in bleeding symptoms.

Both 4-PBA and BIX are reported to have antiapoptotic effects [44–46]. We observed a decreased rate of apoptosis upon treatment with 4-PBA, whereas BIX treatment resulted in a slightly increased rate of apoptosis. A possible explanation for the increased rate of apoptosis seen in BIX-treated cells could be the intracellular accumulation of rFVII-354V-464Hfs causing proteotoxicity. This is supported by the net negative effect on secretion following BIX treatment and the lack of GRP94 induction and relatively low BiP induction compared to 4-PBA. Of note, the only known effects of BIX are as a molecular chaperone inducer, whereas 4-PBA is reported to have many effects, including working both as a chemical chaperone and reducing ER stress [35].

Despite the similarities that we report between the plasma and the recombinant protein, the latter was characterized by very low levels of FXa generation activity. Even the residual function of 4-PBA-induced rFVII-354V-464Hfs was very reduced (0.1% of rFVIIwt), compared to in vivo, where the residual FVII coagulant activity has a median value of approximately 1%. In the stable cell lines used in this study, the FVII:Ag in the conditioned medium was also severely reduced, and no FXaG could be measured in the conditioned medium unless concentrated several folds. The low secretion and clotting activity of this variant in vitro, observed in independent experiments and in different laboratories [13], and even after chaperone treatment, appears to be a feature of the p.A354V-p.P464Hfs variant. In comparison, more than 30 missense changes and 5 nonsense changes have been recombinantly expressed previously with FXaG activity in the conditioned medium comparable to, or even higher, than the FVII coagulant activity measured in circulating plasma. We cannot exclude that there might be unknown factors missing from our artificial system based on overexpression in cells not normally expressing FVII that could stabilize this particular variant.

5. Conclusions

In summary, we provide detailed insights into the variability of the clinical manifestations in patients homozygous for the p.A354V-p.P464Hfs FVII variant, highlighting that genetic components beyond *F7* mutations, together with acquired conditions, may play a key role in this variability. We demonstrate that chemical chaperones can be used as biochemical tools to study the intracellular fate of a Type-II FVII variant with severe clinical manifestations. Even though plasma FVII and rFVII-354V-464Hfs are comparable in size, the latter is characterized by a lower biological activity. Introducing this variant into induced pluripotent stem cells through genome editing followed by differentiation into hepatocytes would constitute a relevant cell model to study the processing of this variant in a context mimicking the natural expression.

Author Contributions: E.A.: Investigation, Writing—original draft, Formal analysis, Validation, Visualization. M.E.C.: Investigation, Writing—original draft, Formal analysis, Validation, Visualization. F.B.: Investigation, Writing—review and editing, Conceptualization. A.B. (Alessio Branchini): Investigation, Writing—review and editing, Visualization. M.B.: Investigation, Writing—original draft, Visualization. G.M.: Investigation, Writing—review and editing. A.D.: Investigation, Data

curation. A.B. (Angelika Batorova): Investigation. E.S.: Investigation, Writing—review and editing, Visualization. C.F.M.: Investigation. G.S.: Writing—review and editing. P.M.S.: Writing—review and editing, Funding acquisition, Supervision. All authors have read and agreed to the published version of the manuscript.

Institutional Review Board Statement: The study was conducted according to the guidelines of the Declaration of Helsinki. The research proposed by the STER Study Group was approved by the Ethics Committee (NCT01269138) of L'Aquila University.

Informed Consent Statement: Informed consent was obtained from all patients at enrolment.

Data Availability Statement: The Seven Treatment Evaluation Registry (STER) prospectively collected data on bleeding episodes, surgery or prophylaxis in patients with FVII deficiency following strictly controlled data collection procedures established by the International FVII Deficiency Study Group [11].

Conflicts of Interest: The authors declare no conflict of interest.

References

1. Kaufman, R.J. Post-translational modifications required for coagulation factor secretion and function. *Thromb. Haemost.* **1998**, *79*, 1068–1079. [CrossRef]
2. Hansson, K.; Stenflo, J. Post-translational modifications in proteins involved in blood coagulation. *J. Thromb. Haemost.* **2005**, *3*, 2633–2648. [CrossRef]
3. Bernardi, F.; Mariani, G. Biochemical, molecular and clinical aspects of coagulation factor VII and its role in hemostasis and thrombosis. *Haematologica* **2021**, *106*, 351–362. [CrossRef]
4. Hagen, F.S.; Gray, C.L.; O'Hara, P.; Grant, F.J.; Saari, G.C.; Woodbury, R.G.; Hart, C.E.; Insley, M.; Kisiel, W.; Kurachi, K.; et al. Characterization of a cDNA coding for human factor VII. *Proc. Natl. Acad. Sci. USA* **1986**, *83*, 2412–2416. [CrossRef] [PubMed]
5. McVey, J.H.; Boswell, E.; Mumford, A.D.; Kemball-Cook, G.; Tuddenham, E.G. Factor VII deficiency and the FVII mutation database. *Hum. Mutat.* **2001**, *17*, 3–17. [CrossRef]
6. Rao, L.V.; Rapaport, S.I. Activation of factor VII bound to tissue factor: A key early step in the tissue factor pathway of blood coagulation. *Proc. Natl. Acad. Sci. USA* **1988**, *85*, 6687–6691. [CrossRef] [PubMed]
7. Mackman, N. The role of tissue factor and factor VIIa in hemostasis. *Anesth. Analg.* **2009**, *108*, 1447–1452. [CrossRef]
8. Girolami, A.; Bertozzi, I.; de Marinis, G.B.; Bonamigo, E.; Fabris, F. Activated FVII levels in factor VII Padua (Arg304Gln) coagulation disorder and in true factor VII deficiency: A study in homozygotes and heterozygotes. *Hematology* **2011**, *16*, 308–312. [CrossRef] [PubMed]
9. Peyvandi, F.; Mannucci, P.M.; Asti, D.; Abdoullahi, M.; Di Rocco, N.; Sharifian, R. Clinical manifestations in 28 Italian and Iranian patients with severe factor VII deficiency. *Haemophilia* **1997**, *3*, 242–246. [CrossRef]
10. Mariani, G.; Lo Coco, L.; Bernardi, F.; Pinotti, M. Molecular and clinical aspects of factor VII deficiency. *Blood Coagul. Fibrinolysis* **1998**, *9* (Suppl. 1), S83–S88.
11. Mariani, G.; Bernardi, F. Factor VII Deficiency. *Semin. Thromb. Hemost.* **2009**, *35*, 400–406. [CrossRef] [PubMed]
12. Perry, D.J. Factor VII Deficiency. *Br. J. Haematol.* **2002**, *118*, 689–700. [CrossRef]
13. Mariani, G.; Herrmann, F.H.; Dolce, A.; Batorova, A.; Etro, D.; Peyvandi, F.; Wulff, K.; Schved, J.F.; Auerswald, G.; Ingerslev, J.; et al. Clinical phenotypes and factor VII genotype in congenital factor VII deficiency. *Thromb. Haemost.* **2005**, *93*, 481–487. [CrossRef] [PubMed]
14. Toso, R.; Pinotti, M.; High, K.A.; Pollak, E.S.; Bernardi, F. A frequent human coagulation Factor VII mutation (A294V, c152) in loop 140s affects the interaction with activators, tissue factor and substrates. *Biochem. J.* **2002**, *363*, 411–416. [CrossRef]
15. Branchini, A.; Baroni, M.; Pfeiffer, C.; Batorova, A.; Giansily-Blaizot, M.; Schved, J.F.; Mariani, G.; Bernardi, F.; Pinotti, M. Coagulationfactor VII variants resistant to inhibitory antibodies. *Thromb. Haemost.* **2014**, *112*. [CrossRef]
16. Arbini, A.A.; Bodkin, D.; Lopaciuk, S.; Bauer, K.A. Molecular analysis of Polish patients with factor VII deficiency. *Blood* **1994**, *84*, 2214–2220. [CrossRef]
17. Wulff, K.; Herrmann, F.H. Twenty two novel mutations of the factor VII gene in factor VII deficiency. *Hum. Mutat.* **2000**, *15*, 489–496. [CrossRef]
18. Fromovich-Amit, Y.; Zivelin, A.; Rosenberg, N.; Tamary, H.; Landau, M.; Seligsohn, U. Characterization of mutations causing factor VII deficiency in 61 unrelated Israeli patients. *J. Thromb. Haemost.* **2004**, *2*, 1774–1781. [CrossRef] [PubMed]
19. Giansily-Blaizot, M.; Rallapalli, P.M.; Perkins, S.J.; Kemball-Cook, G.; Hampshire, D.J.; Gomez, K.; Ludlam, C.A.; McVey, J.H. The EAHAD blood coagulation factor VII variant database. *Hum. Mutat.* **2020**, *41*, 1209–1219. [CrossRef]
20. Herrmann, F.H.; Wulff, K.; Auerswald, G.; Schulman, S.; Astermark, J.; Batorova, A.; Kreuz, W.; Pollmann, H.; Ruiz-Saez, A.; De Bosch, N.; et al. Factor VII deficiency: Clinical manifestation of 717 subjects from Europe and Latin America with mutations in the factor 7 gene. *Haemophilia* **2009**, *15*, 267–280. [CrossRef] [PubMed]

21. Chollet, M.E.; Andersen, E.; Skarpen, E.; Myklebust, C.F.; Koehler, C.; Morth, J.P.; Chuansumrit, A.; Pinotti, M.; Bernardi, F.; Thiede, B.; et al. Factor VII deficiency: Unveiling the cellular and molecular mechanisms underlying three model alterations of the enzyme catalytic domain. *Biochim. Biophys. Acta* **2017**, *1864*, 660–667. [CrossRef] [PubMed]

22. Andersen, E.; Chollet, M.E.; Myklebust, C.F.; Pinotti, M.; Bernardi, F.; Chuansumrit, A.; Skarpen, E.; Sandset, P.M.; Skretting, G. Activation of Endoplasmic Reticulum Stress and Unfolded Protein Response in Congenital Factor VII Deficiency. *Thromb. Haemost.* **2018**, *118*, 664–675. [CrossRef]

23. Triplett, D.A.; Brandt, J.T.; Batard, M.A.; Dixon, J.L.; Fair, D.S. Hereditary factor VII deficiency: Heterogeneity defined by combined functional and immunochemical analysis. *Blood* **1985**, *66*, 1284–1287. [CrossRef] [PubMed]

24. Andersen, E.; Chollet, M.E.; Baroni, M.; Pinotti, M.; Bernardi, F.; Skarpen, E.; Sandset, P.M.; Skretting, G. The effect of the chemical chaperone 4-phenylbutyrate on secretion and activity of the p.Q160R missense variant of coagulation factor FVII. *Cell Biosci.* **2019**, *9*, 69. [CrossRef] [PubMed]

25. den Dunnen, J.T.; Dalgleish, R.; Maglott, D.R.; Hart, R.K.; Greenblatt, M.S.; McGowan-Jordan, J.; Roux, A.F.; Smith, T.; Antonarakis, S.E.; Taschner, P.E. HGVS Recommendations for the Description of Sequence Variants: 2016 Update. *Hum. Mutat.* **2016**, *37*, 564–569. [CrossRef] [PubMed]

26. Goodeve, A.C.; Reitsma, P.H.; McVey, J.H. Nomenclature of genetic variants in hemostasis. *J. Thromb. Haemost.* **2011**, *9*, 852–855. [CrossRef] [PubMed]

27. Hoffman, R.; Benz, E.J., Jr.; Silberstein, L.E.; Heslop, H.; Anastasi, J.; Weitz, J. *Hematology, Basic Principles and Practice*, 5th ed.; Elsevier: Philadelphia, PA, USA, 2018; Chapter 136; pp. 2023–2033.

28. Pinotti, M.; Toso, R.; Redaelli, R.; Berrettini, M.; Marchetti, G.; Bernardi, F. Molecular mechanisms of FVII deficiency: Expression of mutations clustered in the IVS7 donor splice site of factor VII gene. *Blood* **1998**, *92*, 1646–1651. [CrossRef]

29. Barbon, E.; Pignani, S.; Branchini, A.; Bernardi, F.; Pinotti, M.; Bovolenta, M. An engineered tale-transcription factor rescues transcription of factor VII impaired by promoter mutations and enhances its endogenous expression in hepatocytes. *Sci. Rep.* **2016**, *6*, 28304. [CrossRef]

30. Baroni, M.; Martinelli, N.; Lunghi, B.; Marchetti, G.; Castagna, A.; Stefanoni, F.; Pinotti, M.; Woodhams, B.; Olivieri, O.; Bernardi, F. Aptamer-modified FXa generation assays to investigate hypercoagulability in plasma from patients with ischemic heart disease. *Thromb. Res.* **2020**, *189*, 140–146. [CrossRef]

31. Ferrarese, M.; Baroni, M.; Della Valle, P.; Spiga, I.; Poloniato, A.; D'Angelo, A.; Pinotti, M.; Bernardi, F.; Branchini, A. Missense changes in the catalytic domain of coagulation factor X account for minimal function preventing a perinatal lethal condition. *Haemophilia* **2019**, *25*, 685–692. [CrossRef] [PubMed]

32. Katsumi, A.; Senda, T.; Yamashita, Y.; Yamazaki, T.; Hamaguchi, M.; Kojima, T.; Kobayashi, S.; Saito, H. Protein C Nagoya, an elongated mutant of protein C, is retained within the endoplasmic reticulum and is associated with GRP78 and GRP94. *Blood* **1996**, *87*, 4164–4175. [CrossRef]

33. Hayakawa, Y.; Tamura, S.; Suzuki, N.; Odaira, K.; Tokoro, M.; Kawashima, F.; Hayakawa, F.; Takagi, A.; Katsumi, A.; Suzuki, A.; et al. Essential role of a carboxyl-terminal α-helix motif in the secretion of coagulation factor XI. *J. Thromb. Haemost.* **2021**, *19*, 920–930. [CrossRef]

34. Bohm, E.; Seyfried, B.K.; Dockal, M.; Graninger, M.; Hasslacher, M.; Neurath, M.; Konetschny, C.; Matthiessen, P.; Mitterer, A.; Scheiflinger, F. Differences in N-glycosylation of recombinant human coagulation factor VII derived from BHK, CHO, and HEK293 cells. *BMC Biotechnol.* **2015**, *15*, 87. [CrossRef]

35. Kolb, P.S.; Ayaub, E.A.; Zhou, W.; Yum, V.; Dickhout, J.G.; Ask, K. The therapeutic effects of 4-phenylbutyric acid in maintaining proteostasis. *Int. J. Biochem. Cell Biol.* **2015**, *61*, 45–52. [CrossRef] [PubMed]

36. Kasture, A.; Stockner, T.; Freissmuth, M.; Sucic, S. An unfolding story: Small molecules remedy misfolded monoamine transporters. *Int. J. Biochem. Cell Biol.* **2017**, *92*, 1–5. [CrossRef] [PubMed]

37. Chollet, M.E.; Skarpen, E.; Iversen, N.; Sandset, P.M.; Skretting, G. The chemical chaperone sodium 4-phenylbutyrate improves the secretion of the protein CA267T mutant in CHO-K1 cells trough the GRASP55 pathway. *Cell Biosci.* **2015**, *5*, 57. [CrossRef]

38. Pignani, S.; Todaro, A.; Ferrarese, M.; Marchi, S.; Lombardi, S.; Balestra, D.; Pinton, P.; Bernardi, F.; Pinotti, M.; Branchini, A. The chaperone-like sodium phenylbutyrate improves factor IX intracellular trafficking and activity impaired by the frequent p.R294Q mutation. *J. Thromb. Haemost.* **2018**. [CrossRef] [PubMed]

39. Hughes, H.; Stephens, D.J. Assembly, organization, and function of the COPII coat. *Histochem. Cell Biol.* **2008**, *129*, 129–151. [CrossRef] [PubMed]

40. Lee, M.C.; Miller, E.A. Molecular mechanisms of COPII vesicle formation. *Semin. Cell Dev. Biol.* **2007**, *18*, 424–434. [CrossRef] [PubMed]

41. Griffiths, G.; Simons, K. The trans Golgi network: Sorting at the exit site of the Golgi complex. *Science* **1986**, *234*, 438–443. [CrossRef] [PubMed]

42. Hendershot, L.M. The ER function BiP is a master regulator of ER function. *Mt. Sinai J. Med.* **2004**, *71*, 289–297. [PubMed]

43. Vitale, M.; Bakunts, A.; Orsi, A.; Lari, F.; Tade, L.; Danieli, A.; Rato, C.; Valetti, C.; Sitia, R.; Raimondi, A.; et al. Inadequate BiP availability defines endoplasmic reticulum stress. *Elife* **2019**, *8*. [CrossRef]

44. Kudo, T.; Kanemoto, S.; Hara, H.; Morimoto, N.; Morihara, T.; Kimura, R.; Tabira, T.; Imaizumi, K.; Takeda, M. A molecular chaperone inducer protects neurons from ER stress. *Cell Death Differ.* **2008**, *15*, 364–375. [CrossRef]

45. You, Y.D.; Deng, W.H.; Guo, W.Y.; Zhao, L.; Mei, F.C.; Hong, Y.P.; Zhou, Y.; Yu, J.; Xu, S.; Wang, W.X. 4-Phenylbutyric Acid Attenuates Endoplasmic Reticulum Stress-Mediated Intestinal Epithelial Cell Apoptosis in Rats with Severe Acute Pancreatitis. *Dig. Dis. Sci.* **2019**, *64*, 1535–1547. [CrossRef] [PubMed]

46. Yam, G.H.; Gaplovska-Kysela, K.; Zuber, C.; Roth, J. Sodium 4-phenylbutyrate acts as a chemical chaperone on misfolded myocilin to rescue cells from endoplasmic reticulum stress and apoptosis. *Investig. Ophthalmol. Vis. Sci.* **2007**, *48*, 1683–1690. [CrossRef] [PubMed]